

Interaction of the Local Bubble with its environment

Roland Egger

Max-Planck-Institut für extraterrestrische Physik, Giessenbachstrasse,
D-85740 Garching, Germany

Abstract. The Local Bubble (LB), a volume of roughly 100 pc radius filled with ionized gas of high temperature and low density, is not a unique object. It is obviously surrounded by several interstellar bubbles of similar properties. Some of them are as close as to undergo interaction with the LB. Our most prominent neighbour is the Loop I superbubble formed by the Sco-Cen OB association. It is shown that this huge shell is in collision with our Local Bubble. The product of this interaction is an annular cloud of dense neutral gas at the boundary between the two bubbles. Other examples for close neighbouring bubbles are the Gum nebula, the Eridanus bubble and possibly the two radio loops II and III.

1 Introduction

The structure of the diffuse soft X-ray background (SXRb, $E < 2$ keV) has been subject to controversial discussion ever since its discovery by Bowyer et al. (1968). On the one hand there is a very soft (C-band, < 0.3 keV) component which is more or less isotropic at low galactic latitudes ($b < 30^\circ$). This component is obviously not absorbed by any intervening neutral gas with column densities above $N_{\text{H}} = 10^{19} \text{cm}^{-2}$ and therefore, attributable to a local diffuse X-ray source, most probably highly ionized gas filling the Local Bubble (LB). The properties and possible origin of this local interstellar bubble have been determined, modelled and discussed by various authors. A recent review is given by Breitschwerdt (1996) and Breitschwerdt et al. (1996). Two alternative models are either a remnant of a singular supernova event or a fossile superbubble formed by a stellar cluster dissociated long ago. Though the shape of this cavity is not entirely clear, there is general agreement on a mean radius of ~ 100 pc.

At higher galactic latitudes the C-band background is highly structured. This is in principle attributable to two possible origins: Firstly, galactic diffuse sources outside the LB and of varying brightness, shape and size cause strong variations in the measured intensity. Secondly, clouds of intervening neutral material cast shadows on distant diffuse sources. In the energy range above 0.5 keV this shadowing is less severe, apart from the very low latitudes, so that the source distribution is the dominant origin of structure. The two origins can be distinguished using tracers of the N_{H} (21 cm or infrared measurements). All Sky Surveys (e.g. Snowden et al., *this volume*)

show several prominent large scale emission features. Some of them, through their large apparent size on the one hand and through their soft (unabsorbed) X-ray spectrum on the other hand, indicate that they reside in our immediate neighbourhood. Maybe the most impressive one of these is the North Polar Spur (NPS), a huge X-ray arc associated with radio Loop I. For a review of this object see Salter (1983). It has been shown that Loop I is most probably a superbubble formed by the nearby Sco-Cen OB association at ~ 170 pc distance, and that there is evidence for its interaction with the Local Bubble (Egger & Aschenbach 1995). Some details will be discussed below. Other prominent objects of the abovementioned kind are the Monogem Ring (Plucinsky et al. 1996), the Vela supernova remnant (Aschenbach et al. 1995) and the Eridanus X-ray enhancement. At least the latter one is suspected to show indications for an interaction with the LB (Guo et al. 1995). Other candidates for neighbouring interstellar bubbles are found in radio survey maps. The ones with the largest apparent diameters ($\sim 100^\circ$) are the radio loops II and III (Berkhuijsen 1971). These objects have to be very close, unless they have unrealistically large dimensions.

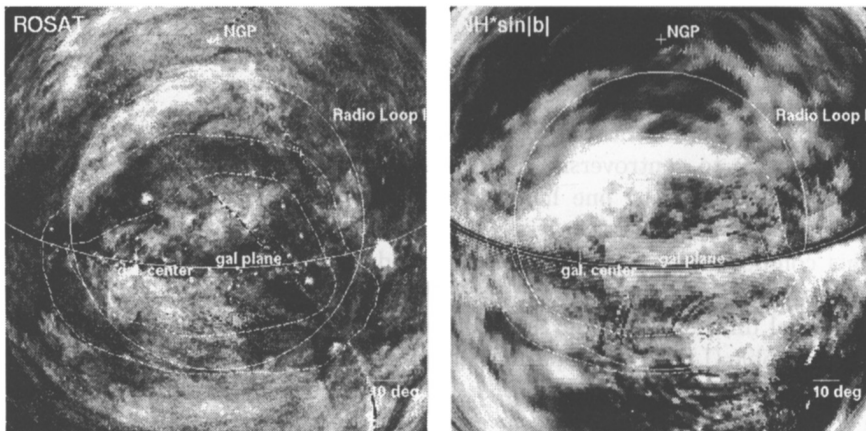


Fig. 1. *Left:* ROSAT Survey map centred on Loop I in the energy range 0.1–2.0 keV. The circle of 58° radius follows the radio continuum loop. The dashed lines outline the contours of the annular shadow. *Right:* HI map divided by $\text{cosec}|b_{II}|$; (see Plate 1).

2 Observations and Results

The ROSAT All Sky Survey in soft X-rays (Trümper 1983) is particularly well suited for studying faint extended sources. This is mainly due to the fast highly resolving X-ray optics (Aschenbach 1988) and the extremely sensitive

low noise detector PSPC (Pfeffermann et al. 1986). The intrinsic angular resolution of the Survey is $1'$ and the energy resolution of $E/\Delta E \sim 2.5$ allows a limited spectral analysis. The data have been cleaned from non-cosmic contaminations, and point-like sources have been removed down to a flux threshold of $6 \times 10^{-14} \text{ ergs cm}^{-2} \text{ s}^{-1}$ (Snowden et al. 1997). Figure 1 (*left*) shows a ROSAT Survey map of $160^\circ \times 160^\circ$ ($E = 0.1 - 2.0 \text{ keV}$) centred on the apparent centre of radio Loop I ($l_{\text{II}} = 329^\circ$, $b_{\text{II}} = +17.5^\circ$) in equal area polar projection. The solid circle outlines a best circle fit to the radio loop of 58° radius. The X-ray morphology appears to be shell-like, well aligned to the radio loop, at least in the region associated with the NPS (upper left in figure 1). The rest appears rather fragmentary. Moreover, there is an elliptical annular shadow obscuring parts of the loop indicated by the dashed lines in figure 1). The ellipse is centred about $l_{\text{II}} = 335^\circ$, $b_{\text{II}} = 0^\circ$. Its long axis is roughly aligned with the galactic plane and has a length of about 127° , while the short axis is about 93° . The width of the ring is 15° on the average.

The right part of figure 1 shows an HI map of the same region (data from Dickey & Lockman 1990). The column densities have been divided by $\text{cosec}|b_{\text{II}}|$ in order to compensate for the contribution of the Galactic disc. This image clearly shows the HI shell with $N_{\text{H}} \sim 10^{20} \text{ cm}^{-2}$ enclosing Loop I at a radius of $\sim 68^\circ$. It also shows a fragmentary ring corresponding to the annular X-ray shadow with column densities up to $\sim 7 \times 10^{20} \text{ cm}^{-2}$.

The central part of the annulus appears to be transparent for the broad X-ray band. Emission from the interior of the Loop I bubble is shining through the ring-shaped absorption feature (left part of figure 1). In the lowest ROSAT energy band R1 (0.1–0.2 keV), however, the interior of the annulus is almost opaque. This indicates the presence of a neutral gas wall of column density $N_{\text{H}} \sim 10^{20} \text{ cm}^{-2}$, which corresponds to optical depth unity in this energy range.

2.1 ROSAT spectra of the North Polar Spur

Three cuts across the X-ray arc defining the North Polar Spur were studied as described in Egger (1993) and Egger (1995). The cuts run roughly along $b_{\text{II}} = 44^\circ$, 34° and 24° . Pulse height spectra were extracted from the PSPC data and analyzed using an absorbed three-component model. One component is the NPS thermal emission, the second component is the LB foreground thermal emission and the third component is an extragalactic power-law spectrum absorbed by the total galactic column density. The parameters of the latter two components were determined within a reference field just outside the emission region of Loop I. For the LB a temperature of $1.2(\pm 0.1) \times 10^6 \text{ K}$ and an emission measure of $3.0 \text{ cm}^{-6} \text{ pc}$ was found, resulting in a particle density of $5.2 \times 10^{-3} \text{ cm}^{-3}$ (assuming collisional ionization equilibrium and a line of sight of 90 pc through the LB in this particular direction). The photon index of the extragalactic power-law component is $\Gamma = -2.5$ and the flux at 1 keV is $12.5 \pm 0.3 \text{ cm}^{-2} \text{ sr}^{-1} \text{ s}^{-1} \text{ keV}^{-1}$ which is in agreement with previous

results (cf. McCammon & Sanders 1990). The spectral studies of the three cuts across the NPS emission resulted in electron temperatures between 2.0 and 3.5×10^6 K and emission measures between 0.02 and $0.04 \text{ cm}^{-6} \text{ pc}$. The absorption values are between 1 and $7 \times 10^{20} \text{ cm}^{-2}$, about a factor of 2–5 below the total column densities in the corresponding directions. Assuming the X-ray NPS to be due to a spherical shock wave of 150 pc radius, shock densities between 0.01 and 0.02 cm^{-3} (increasing from high to low b_{II}) and corresponding electron temperatures between 2.5 and 3.5×10^6 K at the shock front are derived.

3 Discussion

3.1 Loop I – an active superbubble

Stellar activity within the Sco-Cen OB association started $1 - 2 \times 10^7$ years ago (Bertiau 1958). Initially, the strong stellar winds of the young massive stars began to blow a big collective stellar wind bubble filled with hot gas of several 10^6 K. At the time when the massive stars reached their evolutionary time scale ($\sim 4 \times 10^6$ years) a cascade of supernova (SN) explosions began to occur in the interior of the pre-existing cavity taking over the blowing of the bubble from the decaying stellar wind activity. From then on the energy input (by SNe) can be regarded as fairly constant (see e.g. McCray 1987). The increasing lifetime of less massive stars is compensated by their greater number in the initial mass function (IMF) of the stellar cluster. Both follow approximately a power law with index about -1.5 . This goes on until the age of about 5×10^7 years when the least massive stars that still die as SNe have reached the end of their lifetimes

If we now want to estimate the energy input by SNe per time for the present case we have to find out the number of SN explosions that have occurred within the Sco-Cen association up to now. In order to determine the parameters of the IMF we have to restrict ourselves to stars of spectral types later than B1, since these have lifetimes greater than 3×10^7 years and hence, are not affected by loss through SN explosions, yet. Integration of the IMF of the Sco-Cen association between the types B1 ($M \sim 14 M_{\odot}$) and B3 ($M \sim 9 M_{\odot}$), about the least massive stars that still may produce type II SNe, reveals

$$\text{present } N_{\text{B1-3}} = \left[\frac{C \cdot \tilde{M}^{-1.5}}{-1.5} \right]_9^{14} = 42 \quad \Rightarrow \quad C = 3510 \quad (1)$$

where \tilde{M} is the stellar mass in M_{\odot} . The total number of potential SNe is the integral up to the greatest possible masses, earlier than type B3:

$$\text{initial } N_{*} = N_{<\text{B3}} = \left[\frac{3510 \cdot \tilde{M}^{-1.5}}{-1.5} \right]_9^{60} = 82. \quad (2)$$

Since the present number of stars earlier than type B3 is 44, already 38 SNe must have exploded. However, due to small number statistics, the true number may vary by plus or minus 10. Hence, we compute an average SN rate of

$$f_{SN} \approx \frac{82}{5 \times 10^7 \text{ yr}} = \frac{1}{600,000 \text{ yr}} \quad (3)$$

The mechanical luminosity of the SNe is therefore

$$L_{SN} = f_{SN} \cdot E_0 = 5.3 \times 10^{37} \text{ erg/s}, \quad (4)$$

where $E_0 = 10^{51}$ erg is the canonical SN energy.

Now, we have the average “mechanical luminosity” of the stellar association and can handle the problem like a stellar wind blown bubble with a constant energy input per time. McCray & Kafatos (1987) derive the evolution of a superbubble from the stellar wind model of Weaver et al. (1977):

$$R_S = 269 \text{ pc} \left(\frac{L_{38}}{n_0} \right)^{1/5} t_7^{3/5} \quad V_S = 16 \text{ km s}^{-1} \left(\frac{L_{38}}{n_0} \right)^{1/5} t_7^{-2/5} \quad (5)$$

and thus,

$$R_S = 17 V_S t_7. \quad (6)$$

Here, R_S is the radius of the radiative shell in pc, V_S is its expansion velocity in km s^{-1} and t_7 the age of the bubble in 10^7 years. The model is compatible with the data of Loop I, if the age is about 10^7 years and the present expansion velocity is about 10 km s^{-1} . This is consistent with the literature quoted in the introduction where values between $V_S = 2 \text{ km s}^{-1}$ and $V_S = 40 \text{ km s}^{-1}$ can be found. Also the interior structure of the superbubble is similar to that of a stellar wind bubble in the radiative stage:

$$n_i \approx 1.5 \times 10^{-3} \text{ cm}^{-3} (N_* E_{51})^{0.2} n_0^{0.5} t_7^{-0.6} \left(1 - \frac{r}{R_S} \right)^{-0.4} \quad (7)$$

$$T_i \approx 1.1 \times 10^6 \text{ K} (N_* E_{51})^{0.2} n_0^{0.1} t_7^{-0.2} \left(1 - \frac{r}{R_S} \right)^{0.4} \quad (8)$$

where n_i , T_i are interior density and temperature, n_0 is the density of the surrounding interstellar medium and E_{51} is the energy of a single supernova in units of 10^{51} erg (McCray & Kafatos, 1987). The measured column density of the HI shell around Loop I is $\sim 10^{20} \text{ cm}^{-2}$. With a shell radius of $R_S = 158$ pc this gives an initial ambient density of $n_0 \sim 0.63 \text{ cm}^{-3}$. For comparison: Dickey & Lockman (1990) find an average density in the galactic plane of 0.57 cm^{-3} . Hence, the central density of the Loop I bubble would be $\sim 3 \times 10^{-3} \text{ cm}^{-3}$ which holds for a major fraction of the interior, while the central temperature would be $\sim 2.5 \times 10^6$ K.

The observed shell radius of 160 pc is by about 40 % smaller than the one predicted by the model. This can by no means be attributed to small

variations of any of the contributing parameters, since their powers are so low. A possible explanation would be confinement by the ambient magnetic field. This is supported by the strong synchrotron radiation associated with Loop I that indicates field strengths of at least $B_0 = 5 \mu\text{G}$. Slavin & Cox (1992) show, that bubbles in an ambient field of $5 \mu\text{G}$ have radii 30–50% smaller than those in an unmagnetized medium. Another possible reason for the smaller radius could be loss of interior thermal energy by mass load due to cloud evaporation (McKee & Ostriker 1977). Support is given to this view by the observation of clouds in the interior of Loop I (e.g. the R CrA complex, Wang, 1994) which, by their cometary shapes, actually show evidence for the interaction with blast waves from Sco-Cen supernovae.

The latest supernova that occurred within the Sco-Cen association must have produced a shock wave that crossed the hot tenuous interior rapidly until it was decelerated at the steep density gradient near the dense walls of the bubble. The result was heating the bubble walls to temperatures of $3\text{--}4 \times 10^6$ K giving rise to the prominent X-ray feature of the North Polar Spur. It is reasonable to assume that the shock front has hit the walls no longer than 10^4 years ago, since, otherwise radiative cooling would have caused it to disappear out of the X-ray band. SNR evolution in a hot ambient medium is described by an expansion law like

$$\frac{V_S}{C_0} \propto \left(\frac{R_S}{R_0} \right)^{-3/2}, \quad (9)$$

where C_0 is the sound velocity and $R_0 \propto E_0/p_0$ is a characteristic radius (p_0 is the ambient pressure) (Gaffet 1978). It can be shown (see Egger 1994 and Egger 1995) that the temperatures and densities deduced from the X-ray observations are compatible with a supernova of $\sim 10^{51}$ erg that occurred somewhere within the Sco-Cen association about 2×10^5 years ago.

3.2 Interaction with the LB

If we consider the geometrical facts compiled in the introduction, it becomes obvious that the LB and the Loop I bubble have to have undergone some kind of interaction. A proof for the actual case of such an interaction is given by the annular X-ray shadow described above. An annular volume of dense neutral gas is predicted to form at the interaction zone between two colliding interstellar bubbles. Hydrodynamical computations (e.g. Yoshioka & Ikeuchi 1990) reveal that the density within the cool interaction ring is by a factor of 20 to 30 higher than that of the ambient medium. The observed neutral gas ring appears to be somewhat distorted and incomplete which may be due to deviations from spherical symmetry of either the LB or the Loop I superbubble or both. Apart from this, it resembles quite well the simulated scenario of the two colliding shells as seen from inside one of the two bubbles looking towards the other one (figure 2).

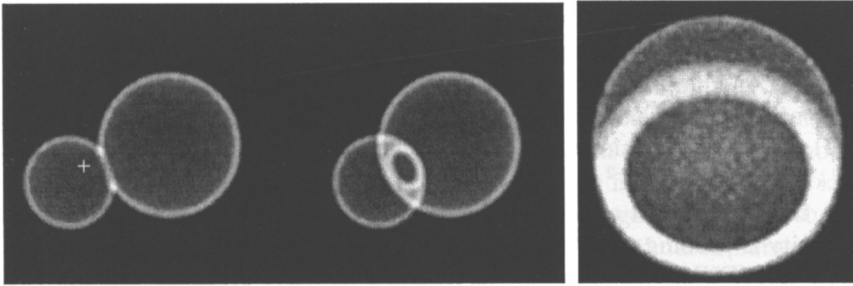


Fig. 2. *Left* : Projected column density of a simulation of two colliding bubbles seen from aside. *Middle* : The same, rotated by 30° . *Right* : The same as seen from inside. The viewing point is marked by the cross in the left image. The viewing direction is towards the larger bubble.

The distance of the interaction feature can be estimated by absorption line studies of nearby stars which are projected on the ring (figure 3, data compiled by Fruscione et al. 1994). It is found that the N_H jumps from less than 10^{20}cm^{-2} to more than $7 \times 10^{20}\text{cm}^{-2}$ near the distance of about 70 pc which places the dense gas between the LB and Loop I. The column density allows to estimate a particle density within the ring of $n \sim 15\text{cm}^{-3}$. This exceeds the ambient density ($n_0 \sim 0.6\text{cm}^{-3}$) by a factor of 25, in good agreement with the theoretical prediction.

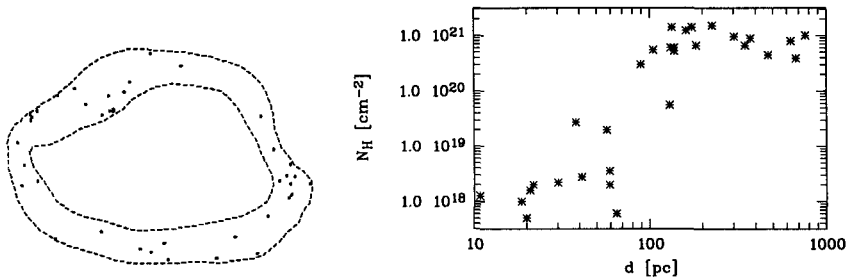


Fig. 3. *Left*: Positions of stars projected on the annular X-ray shadow. *Right*: HI column densities towards stars projected on the interaction ring. N_H rises to $\sim 7 \times 10^{20}\text{cm}^{-2}$ near the distance of about 70 pc.

3.3 The wall

The simulations mentioned above also show that, if at least one of the bubbles has already reached the radiative stage of evolution prior to the collision, the

two interiors would not merge but a dense wall would form between the bubbles. This corresponds to the observation that the interior of the HI ring is almost opaque in the R1 band. Further support is given by optical and UV spectral analysis of stars near the centre of Loop I (Centurion & Vladilo 1991). These observations reveal evidence for the presence of a neutral gas wall of $N_H \sim 10^{20} \text{cm}^{-2}$ at a distance of 40 ± 25 pc.

A totally different approach to investigating the size and shape of the local cavity is probing the extinction of the interstellar medium in the extreme ultraviolet (EUV, 0.05–0.2 keV) by differential source counts. Warwick et al. (1993) performed such an analysis making use of the ROSAT Wide Field Camera source catalogue. They found that the apparent brightness and distribution of the EUV sources (mainly white dwarfs and late type stars) is compatible with a local cavity of 80 pc mean radius. There are two exceptional directions where the source counts indicate larger distances to the walls: the regions about $l_{\text{II}} = 200^\circ$, $b_{\text{II}} = -30^\circ$ (≈ 100 pc) and $l_{\text{II}} = 120^\circ$, $b_{\text{II}} = +45^\circ$ (≈ 120 pc). There is, however, a field on the sky that nearly exactly matches the region described above as the annular X-ray shadow, which is almost completely devoid of sources in the EUV band below 0.1 keV. This result again indicates the presence of a dense HI wall in the direction of Loop I that could be even as close as 10 pc.

It is still under discussion, if the interior of the LB is hot or warm or only lukewarm (see e.g. Breitschwerdt, *this volume*). In any case, the ongoing supernova activity within Loop I makes the pressure at least twice as high as that in the LB, even if we adopt the canonical $T_{\text{LB}} = 10^6$ K. This overpressure would cause the wall at the interaction zone bending and moving slowly towards us. The nearest part of it may have come already fairly close to the solar position (10–40 pc). Moreover, one would expect a gas “wall” of ~ 1 pc thickness and a density of $20\text{--}30 \text{cm}^{-3}$ to be unstable on a time scale of about 10^6 years (Kahn, F.D., *private communication*). A more thorough study of this aspect (Breitschwerdt & Egger, 1997) reveals the possibility of instabilities on the parsec scale. As long as the pressure driven state continues, the wall would not disintegrate but cloudlets of parsec size could be expelled from the instabilities towards the interior of the LB. Thus, it is likely that the Local Cloud or the Local Fluff of neutral gas surrounding the Sun within the next 10 pc (see e.g. Lallement, *this volume*) are a product of the interaction zone between Loop I and the LB.

3.4 Other bubbles in our neighbourhood

The Eridanus X-ray enhancement is also discussed to be a superbubble formed by the activity of young stars (Guo et al. 1995). The molecular gas associated with the near side of this bubble is only 160 pc away and its velocity structure suggests possible interaction with the LB. The Monogem Ring is a soft X-ray emitting shell of 25° diameter. Estimates of the distance to the centre vary between 300 and 1300 pc. Therefore, size and energy content

are equally uncertain (Plucinsky et al. 1996). Though it is very close, the Monogem Ring seems not to be an immediate neighbour and any interaction with the LB is doubtful. The Vela supernova remnant has been shown to be embedded in a hot bubble confined by a shell associated with the Gum Nebula (Aschenbach et al. 1995). The X-ray spectrum of this “Gum-Bubble” reveals an equilibrium temperature of $\sim 10^6$ K. This is confirmed by a kinematic analysis of supernova explosion fragments propagating through the hot ambient medium. The distance to the Vela pulsar is estimated between 300 and 500 pc. The lower limit would place the near side of the “Gum-Bubble” close to the LB boundary. This is supported by the observation that the absorbing column density towards the Vela SNR is only about 10^{20}cm^{-2} .

The giant radio loops II, III and IV are other candidates for possible nearby superbubbles. Nowhere, however, is the situation as clear as in the case of Loop I. No obvious X-ray enhancement is associated with either of them. Loop IV is the only one that seems to be associated at least with an HI arc. This Loop is seen in projection through the interior of Loop I and therefore, it is most probably behind it. Loops II and III are nearly as large in apparent size as Loop I and therefore, probably close. However, they are crossing each other and thus, only one of them can be regarded as our immediate neighbour. It is however remarkable, that Loop II seems to be associated with a huge bulk of HI apparently filling the whole loop. This HI corresponds to a depression in the soft X-ray background. Possibly, it is due to neutral gas compressed between the LB and a fossil superbubble. This wall of neutral gas, on the other hand, would hinder any observation of X-ray emission if the interior of the neighbour bubbles is at equilibrium temperatures less or equal 10^6 K. This is subject of an ongoing study.

4 Conclusion

The solar neighbourhood is located within an interstellar bubble probably filled with hot gas of low density. The LB seems to be surrounded by numerous bubbles of similar properties. At least a few of them are filled with hot X-ray emitting gas due to ongoing stellar activity. The picture suggested by the observations is that of a “Local Interstellar Foam” made up of seven or more bubbles close to each other. It is well possible that this “foam” is associated with the local region of stellar activity defined as *Gould’s Belt*. This indicates a high local filling factor of hot gas, maybe up to 50 %.

Acknowledgements

I would like to thank the referee for useful comments and hints. The ROSAT project has been supported by the German Bundesministerium für Zukunft (BMBF/DLR) and the Max-Planck-Gesellschaft (MPG).

References

- Aschenbach, B., *Applied Optics* **27** (1988) 1404
 Berkhuijsen, E.M., *A.A.* **14** (1971) 359
 Bertiau, F.C., Bertiau, S.J., *ApJ* **128** (1958) 533
 Centurion, M., Vladilo, G., *ApJ* **372** (1991) 494
 Bowyer, C.S., Field, G.B., *Nature* **217** (1968) 32
 Breitschwerdt, D., *Space Science Reviews* **78** (1996) 173
 Breitschwerdt, D., Egger, R.J., Freyberg, M.J., Frisch, P.C., Vallerga, J.V., *Space Science Reviews* **78** (1996) 183
 Breitschwerdt, D., Egger, R.J., A.A. (1997) (*in preparation*)
 Dickey J.M., Lockman, F.J., *ARA&A* **28** (1990) 215
 Egger, R.J., MPE Report **249** (1993) ISSN 0178-0719
 Egger, R.J., 1995 in *The Physics of the interstellar medium and the intergalactic medium*, eds.: A. Ferrara, C. Heiles, C.F. McKee, P. Shapiro, *Pub. Astron. Soc. of the Pacific Conf. Ser.* **80** (1995) 45
 Egger, R.J., Aschenbach, B., A.A. **294** (1995) L25
 Fruscione, A., Hawkins, I. Jelinsky, P., Wiercigroch, A., *ApJ suppl.* **94** (1994) 127
 Gaffet, B., *ApJ* **225** (1978) 442
 Guo, Z., Burrows, D.N., Sanders, W.T., Snowden, S.L., Penprase, B.E., *ApJ* **453** (1995) 256
 McCammon, D., Sanders, W.T., *ARA&A* **28** (1990) 657
 McCray, R. in *Spectroscopy of astrophysical plasmas*, eds. A. Dalgarno, D. Layzer, *Cambridge Astrophys. Series*, Cambridge Univ. Press (1987) 255
 McCray, R., Kafatos, M., *ApJ* **317** (1987) 190
 McKee, C.F., Ostriker, J.P., *ApJ* **218** (1977) 148
 Pfeffermann E., Briel, U.G., Hippmann, H. et al., *Proc. SPIE*, **733** (1986) 519
 Plucinsky, P.P., Snowden, S.L., Aschenbach, B., Egger, R.J., Edgar, R., McCammon, D., *ApJ* **463** (1996) 224
 Salter, C.J., *Bull. Astr. India* **11** (1983) 1
 Slavin, J.D., Cox, D.P., *ApJ* **392** (1992) 131
 Snowden, S.L., Egger, R.J., Freyberg, M.J. et al., *ApJ* **485** (1997) 125
 Trümper, J., *Adv. Space Res.* **4** (1983) 241
 Wang, Q.D., in *The Soft X-Ray Cosmos*, AIP Conference Proceedings, eds. Schlegel, E.M., Petre, R., (1983) (New York, AIP) 301
 Warwick, R.S., Barber, C.R., Hodkin, S.T., Pye, J.P., *M.N.R.A.S.* **262** (1993) 28
 Weaver, R., McCray, R., Castor, J., Shapiro, P., Moore, R., *ApJ* **218** (1977) 377
 Yoshioka, S., Ikeuchi, S., *ApJ* **360** (1990) 352